1-1-2018

Strength of π-Stacking, from Neutral to Cation: Precision Measurement of Binding Energies in an Isolated π-Stacked Dimer

Damian Kokkin
Marquette University

Maxim V. Ivanov
Marquette University

John Loman
Marquette University

Jin-Zhe Cai
Marquette University

Rajendra Rathore
Marquette University, rajendra.rathore@marquette.edu

See next page for additional authors

Accepted version. *The Journal of Physical Chemistry Letters*, Vol. 9, No. 8 (2018): 2058-2061. DOI.

Strength of π-Stacking, from Neutral to Cation: Precision Measurement of Binding Energies in an Isolated π-Stacked Dimer

Damian Kokkin
Department of Chemistry, Marquette University, Milwaukee, WI
Maxim V. Ivanov
Department of Chemistry, Marquette University, Milwaukee, WI
John Loman
Department of Chemistry, Marquette University, Milwaukee, WI
Jin-Zhe Cai
Department of Chemistry, Marquette University, Milwaukee, WI
Rajendra Rathore
Department of Chemistry, Marquette University, Milwaukee, WI
Scott A. Reid

Department of Chemistry, Marquette University, Milwaukee, WI

Abstract

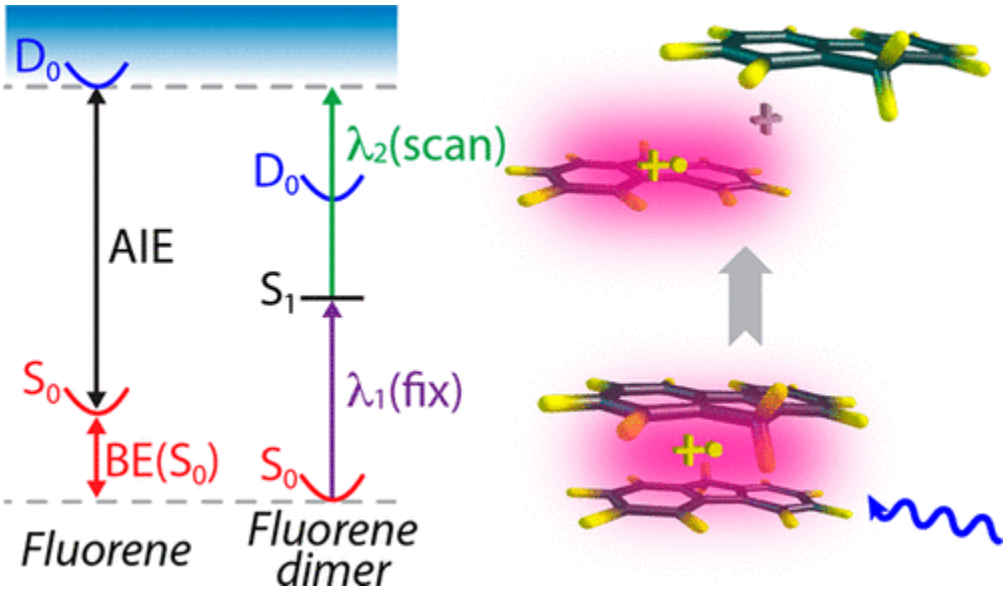

π-Stacking interactions are ubiquitious across chemistry and biochemistry, impacting areas from organic materials and photovoltaics to biochemistry and DNA. However, experimental data is lacking regarding the strength of π-stacking forces—an issue not settled even for the simplest model system, the isolated benzene dimer. Here, we use two-color appearance potential measurements to determine the binding energies of the isolated, π-stacked dimer of fluorene ($C_{13}H_{10}$) in ground, excited, and ionic states. Our measurements provide the first precise values for π-stacking interaction energies in these states, which are key benchmarks for theory. Indeed, theoretical predictions using ab initio and carefully benchmarked DFT methods are in excellent agreement with experiment.

Noncovalent interactions are crucially important in diverse areas extending from organic materials to drug–substrate interactions to protein folding. Of these forces, π-stacking is not the strongest, yet its importance in systems involving aromatic residues is increasingly recognized. For example, dimer radical cations have been extensively investigated in the context of understanding charge transport processes in π-stacked assemblies and DNA and nucleobase oxidative damage.[1–5]

Despite the importance of π-stacking, few studies have examined the strength of the binding interaction in isolated dimers; these are summarized in a recent review.[6] Experimental measurements of the ground state binding energy of the prototypical system, the benzene dimer, vary by some 50%,[7–9] roughly bracketing the best theoretical predictions.[10–13] Even for the few systems that have been studied,[6] it is not clear that a π-stacked arrangement is favored in the ground state as C–H/π interactions are also prevalent. In such cases, excited/ionic state barriers to conformational reorganization may also limit access to π-stacked structures. Yet, experimental studies of π-stacking interactions are critical for providing benchmark data for theoretical methods as commonly employed computational methods (e.g., DFT) can exhibit deficiencies in the proper treatment of dispersion.[14,15]

To address this issue, here we report new experimental studies of a model π-stacked system, the isolated fluorene ($C_{13}H_{10}$) van der Waals dimer $(F)_2$, using two-color appearance potential[16–20] (2CAP) measurements. Extensive measurements of the electronic spectra and threshold ionization potentials (IPs) of the monomer and dimer[21–23] have determined the energies of ground (S_0), excited (S_1), and cation radical (D_0) states to spectroscopic accuracy, as illustrated in Figure 1. With this information in hand, the binding energies in all three states are simply derived, through the thermochemical cycles shown in Figure 1, from the measurement of the binding energy in any one state, which links the respective ladders. We achieve this by measuring the fragmentation of the isolated dimer cation radical in a cold supersonic beam, determining the binding energy in S_0 using the 2CAP method.

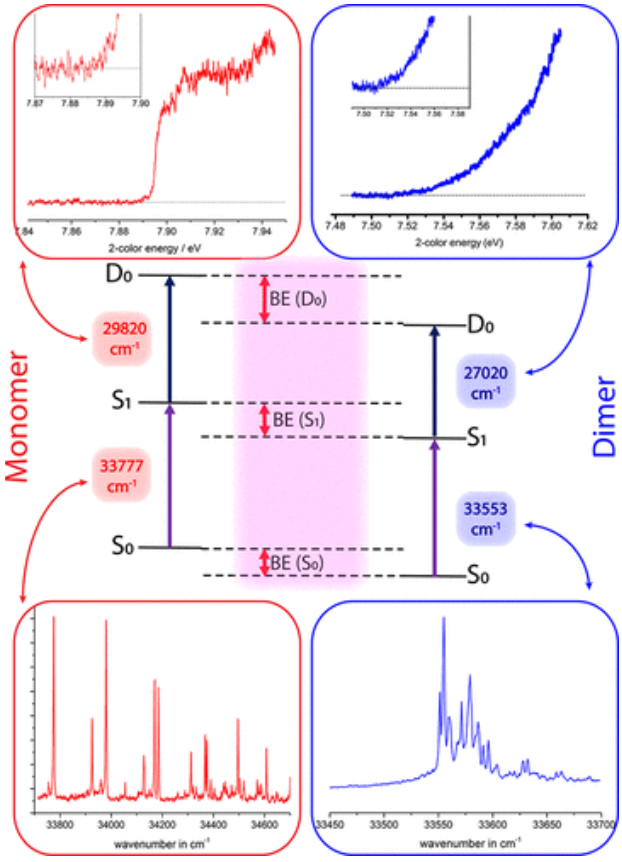

Figure 1. Schematic of thermochemical cycles used to connect energies of ground, excited, and cation radical states. The energy ladders for the monomer and dimer have been determined to spectroscopic accuracy.

Use of the thermochemical scheme in Figure 1 is strictly appropriate only if adiabatic IPs are measured.[6] This is certainly true for the monomer, as evidenced by the abrupt onset in the ion yield curve (inset of Figure 1), signifying a small geometry change between excited and cation radical states. For the dimer, we have shown that the ground state structure and corresponding excited state structure accessed by vertical excitation correspond to a parallel-orthogonal π-stack, as evidenced by two excitonic components of nearly equal intensity in the excitation spectrum (Figure 1, lower right). However, the line widths in this spectrum are homogeneously broadened, indicating a rapid (~2 ps) rearrangement (to a sandwich excimeric structure as evidenced in a broad, unstructured, and red-shifted emission band) in the excited state.[22] As our two-color resonant ionization method features a

time delay of tens of ns, ionization occurs only from the excimer well, which is structurally similar to the dimer cation radical. Thus, we conclude that our measured IP of the dimer must also be close to the adiabatic value, a point examined further below.

We determined the S_0 binding energy using 2CAP measurements, which give an upper limit to the binding energy.[16] In this method, shown schematically in Figure 2a with details provided in the Supporting Information, two-color excitation prepares the dimer cation with a well-defined energy, and the yield of the (fragment) monomer cation is measured as the ionizing laser is scanned. The disadvantage of this method is that the excess energy taken away by the electron at threshold is not known.[6] Recent studies of a related system, the anisole dimer,[16,24] illustrate that in comparison with velocity mapped ion imaging (VMI) measurements, the more sensitive 2CAP method is preferred when fragmentation preferentially populates excited (vibrational or electronic) states.

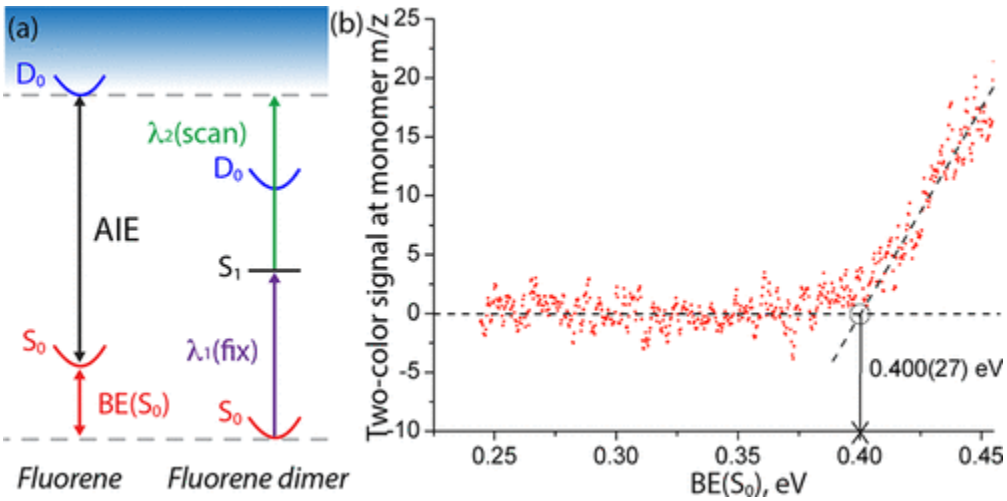

Figure 2. (a) Schematic of the 2CAP method. (b) 2CAP measurement of the ground state binding energy of the fluorene dimer.

Figure 2b displays the 2CAP curve, obtained by tuning λ_1 (panel (a)) to the dimer origin and scanning λ_2 while monitoring the monomer mass channel. The energy axis is given in eV and is determined by subtracting the monomer ionization energy from the two-photon excitation energy. A clear onset is observed, and a linear extrapolation of the rising edge to the baseline returns a value of $E_{binding}$ (in S_0) = 0.400(27) eV. Application of the thermochemical cycle (Figure 1) then affords the binding energy in excited (S_1) and cation radical (D_0) states, given in Table 1 in units of kJ/mol. We note that the binding energy in D_0 is roughly twice that in S_0. It may seem surprising that the binding energies in S_0 and S_1 are similar; however, remember that here we measure the binding energy of a local (parallel-orthogonal) minimum accessed upon vertical electronic excitation, not the global minimum in S_1, which is the sandwich excimer and is more strongly bound.[22]

Table 1. Comparison of Experimental and Computed Binding Energies[a]

	binding energy in kJ/mol		
method	**S_0**	**S_1**	**D_0**
experiment (2CAP)	38.6(26)	41.2(26)	74.7(28)
CAM-B3LYP-D3/6-31G(d)	34.2	41.5	77.5
CAM-B3LYP-D3/cc-pVDZ	36.6	43.9	78.9
B1LYP40-D3/6-31G(d)[b]	26.9	35.5	72.6
B1LYP40-D3/cc-pVDZ[b]	28.3	37.5	73.9
PBE0-D3/def2-SV(P)	40.1	61.2	100.5
PBE0-D3/cc-pVDZ	41.2	62.5	99.7
M06-2X/6-31G(d)	33.0	43.6	88.2
M06-2X/cc-pVDZ	40.8	51.4	92.9
EOM-CCSD/6-31G(d)[c]	29.7	31.7	76.6
EOM-CCSD/cc-pVDZ[c]	34.5	37.2	83.1

[a] All DFT binding energies were corrected for zero-point energy and basis set superposition error using the counterpoise method.

[b] Dispersion parameters from CAM-B3LYP-D3 method were employed.

[c] Single-point calculations at CAM-B3LYP-D3-optimized geometries: CCSD for ground states, EOM-EE-CCSD for excited states, EOM-IP-CCSD for cation radical states.

How do the experimental values compare with theory? Previously, we[22] and others[25] have reported benchmarking studies of the neutral benzene dimer and related complexes using DFT and ab initio methods. This work showed that a simple PBE0 functional,[26,27] augmented with Grimme's D-3 dispersion correction,[28] performed well. For cation radical states, our prior work has established that a B1LYP functional[29] with 40% contribution from the exact Hartree–Fock exchange (i.e., B1LYP40) is a method of choice for predicting cationic charge stabilization/delocalization in π-conjugated systems.[30,31] Building upon these efforts, we have performed a benchmark DFT study of the fluorene dimer in ground, excited, and cation radical states. All DFT calculated binding energies were corrected for the zero-point energy and basis set superposition error using the counterpoise method.[32,33] Taking the DFT-optimized structures, we then performed single-point ab initio calculations. In order to obtain reliable values of the binding energies at the neutral, excited, and cation radical states, the method of choice must treat all three electronic states on the same footing. We therefore resorted to the equation-of-motion coupled-cluster (EOM-CCSD) family of methods,[34] i.e., EOM-EE-CCSD for the excited state, EOM-IP-CCSD for the cation radical state, and CCSD for neutral state. Due to the computational restraints, all calculations were performed with 6-31G(d) and cc-pVDZ basis sets.[35,36]

Table 1 provides a comparison of experiment and selected theoretical values, in kJ/mol; the full results of this initial benchmarking study are provided in Table S2 in the Supporting Information. Note that according to the experiment calculated binding energies at ground and excited states are referenced to

the parallel-orthogonal π-stacked structure, while the binding energy at the cation radical state corresponds to the sandwich structure (Figure 3A). Overall, CAM-B3LYP-D3[37] best reproduces the experimental binding energies across all three states, while B1LYP40-D3 provides the most accurate description of the cation radical state. In contrast, the PBE0-D3 and M06-2X[38] methods well reproduce the binding in S_0 but severely overestimate binding in excited and especially in the cation radical states. A proper theoretical prediction of π-stacked dimer cation radicals using DFT must account for the self-interaction error and dispersion interaction in a balanced way. Remarkably, despite modest basis sets, EOM-CCSD calculations performed exceedingly well by providing a balanced description of the binding energies across all three states.

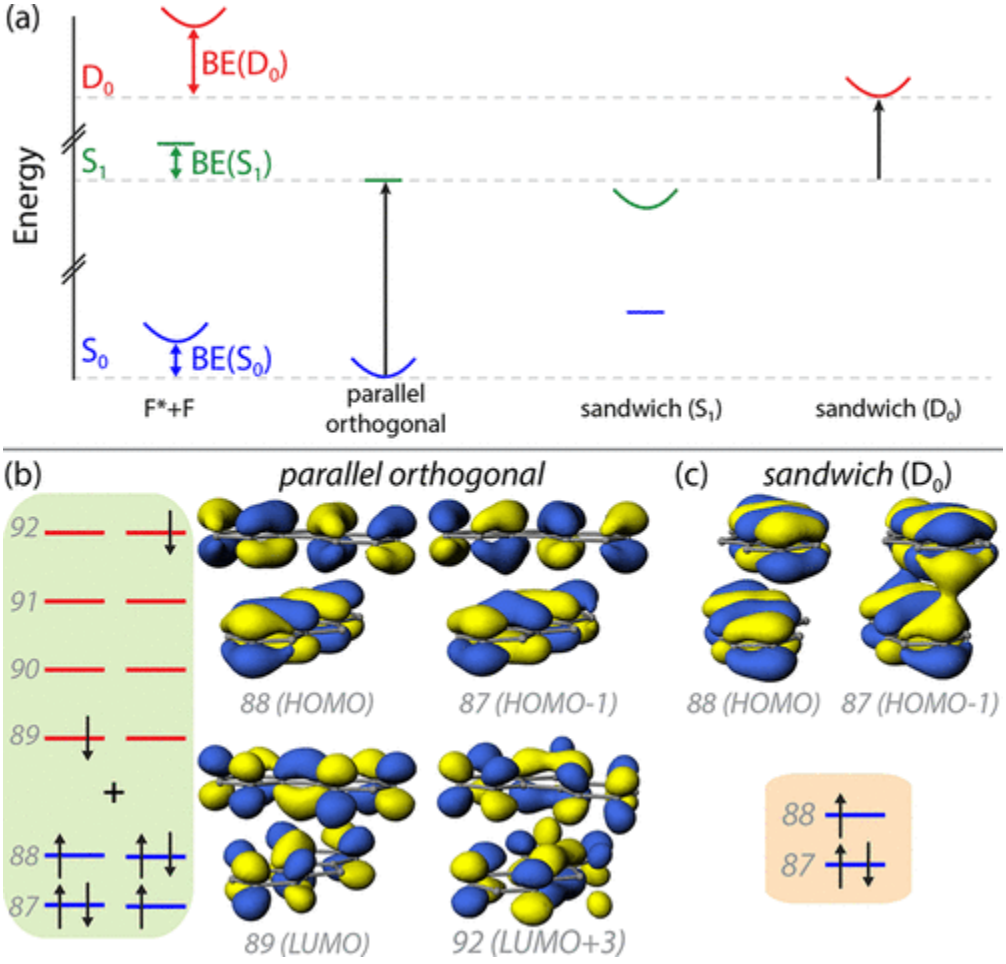

Figure 3. (a) Schematic representation of the relevant points on the PES of the fluorene dimer at neutral (S_0), excited (S_1), and cation radical (D_0) states. (b) Leading electronic configurations of the excited $(F)_2$ at parallel-orthogonal geometry with corresponding MOs involved in the excitation computed using EOM-EE-CCSD/cc-pVDZ (see Table S1 in the Supporting Information for all configurations). (c) Dominant configuration of the ionized $(F)_2$ at sandwich geometry with corresponding MOs computed using EOM-IP-CCSD/cc-pVDZ.

Considering the molecular orbital description of the electronic structure of the fluorene dimer, the upper two occupied frontier molecular orbitals (FMOs) are formed as symmetric (HOMO–1) and antisymmetric (HOMO) linear combinations of the fluorene HOMOs. In parallel-orthogonal $(F)_2$, the

orthogonal arrangement of the monomeric HOMOs leads to poor orbital overlap and results in an almost nonexistent HOMO/HOMO–1 energy gap of 0.03 eV. The first excited state of parallel-orthogonal $(F)_2$ is dominated by the similarly contributing transitions from HOMO and HOMO–1 to LUMO and LUMO+3, respectively (Figure 3B and see Table S1 in the Supporting Information for details on all transitions involved in the excitation).

In sandwich-like $(F)_2$, i.e., the global minimum structure at the D_0 state, cofacial arrangement of two fluorenes results in a significant orbital overlap and, consequently, in a sizable HOMO/HOMO–1 energy gap of 1.1 eV. The ionized state of sandwich-like $(F)_2$ is dominated by the Koopmans-like configuration corresponding to electron ejection from the HOMO (Figure 3C).

Note that a different relative arrangement of fluorenes in S_0 and (vertical) S_1 states as compared to the D_0 state (i.e., orthogonal vs sandwich) results in the different electronic coupling as judged by the different HOMO/HOMO–1 energy gap and, as such, explains the remarkably similar BEs in S_0 and S_1 states that are nearly by a factor of 2 smaller than that in the D_0 state (Table 1). Again, we emphasize that the parallel-orthogonal S_1 structure is accessed via vertical excitation from the ground state and corresponds to a local minimum.

In conclusion, we have reported precise measurement of the binding energies of an isolated π-stacked dimer, the van der Waals dimer of fluorene, in its ground, excited, and cation radical states using 2CAP measurements. The derived values are in excellent agreement with ab initio and benchmarked DFT calculations, with CAM-B3LYP-D3 best reproducing, even using the modest basis sets (with counterpoise correction), the experimental binding energies across all three states. The B1LYP functional with 40% Hartree–Fock exchange, optimized to describe cationic charge delocalization in π-conjugated systems, provides an accurate description of the cation radical state.

Supporting Information

The Supporting Information is available free of charge on the ACS Publications website at DOI: 10.1021/acs.jpclett.8b00742.

The authors declare no competing financial interest.

Acknowledgments

Support by the National Science Foundation (Grant CHE-1508677) is acknowledged. The calculations were performed on the high-performance computing cluster Père at Marquette University funded by NSF Awards OCI-0923037 and CBET-0521602 and the Extreme Science and Engineering Discovery Environment (XSEDE) funded by NSF (TG-CHE130101).

References

1 Prat, F.; Houk, K. H.; Foote, C. Effect of Guanine Stacking on the Oxidation of 8-Oxoguanine in B-DNA. *J. Am. Chem. Soc.* 1998, *120*, 845– 846, DOI: 10.1021/ja972331q

2 Sugiyama, H.; Saito, I. Theoretical Studies of GG-Specific Photocleavage of DNA Via Electron Transfer: Significant Lowering of Ionization Potential and 5â-Localization of HOMO of Stacked GG Bases in B-Form DNA. *J. Am. Chem. Soc.* 1996, *118*, 7063– 7068, DOI: 10.1021/ja9609821

3 Zadorozhnaya, A. A.; Krylov, A. I. Ionization-Induced Structural Changes in Uracil Dimers and Their Spectroscopic Signatures. *J. Chem. Theory Comput.* 2010, *6*, 705– 717, DOI: 10.1021/ct900515a

4 Schumm, S.; Prevost, M.; Garcia-Fresnadillo, D.; Lentzen, O.; Moucheron, C.; Kirsch-De Mesmaeker, A. Influence of the Sequence Dependent Ionization Potentials of Guanines on the Luminescence Quenching of Ru-Labeled Oligonucleotides: A Theoretical and Experimental Study. *J. Phys. Chem. B* 2002, *106*, 2763– 2768, DOI: 10.1021/jp013185k

5 Bravaya, K. B.; Kostko, O.; Ahmed, M.; Krylov, A. I. The Effect of Pi-stacking, H-bonding, and Electrostatic Interactions on the Ionization Energies of Nucleic Acid Bases: Adenine-adenine, Thymine-thymine and Adenine-thymine Dimers. *Phys. Chem. Chem. Phys.* 2010, *12*, 2292– 2307, DOI: 10.1039/b919930f

6 Frey, J. A.; Holzer, C.; Klopper, W.; Leutwyler, S. Experimental and Theoretical Determination of Dissociation Energies of Dispersion-Dominated Aromatic Molecular Complexes. *Chem. Rev.* 2016, *116*, 5614– 5641, DOI: 10.1021/acs.chemrev.5b00652

7 Krause, H.; Ernstberger, B.; Neusser, H. J. Binding Energies of Small Benzene Clusters. *Chem. Phys. Lett.* 1991, *184*, 411– 417, DOI: 10.1016/0009-2614(91)80010-U

8 Grover, J. R.; Walters, E. A.; Hui, E. T. Dissociation Energies of the Benzene Dimer and Dimer Cation. *J. Phys. Chem.* 1987, *91*, 3233– 3237, DOI: 10.1021/j100296a026

9 Nishiyama, I.; Hanazaki, I. Infrared Photodissociation of the Benzene Dimer. Translational Energy Distribution of Dissociation Fragments. *Chem. Phys. Lett.* 1985, *117*, 99– 102, DOI: 10.1016/0009-2614(85)85214-3

10 Sherrill, C. D.; Takatani, T.; Hohenstein, E. G. An Assessment of Theoretical Methods for Nonbonded Interactions: Comparison to Complete Basis Set Limit Coupled-cluster Potential Energy Curves for the Benzene Dimer, the Methane Dimer, Benzene- Methane, and Benzene- H2S. *J. Phys. Chem. A* 2009, *113*, 10146– 10159, DOI: 10.1021/jp9034375

11 Gonthier, J. F.; Sherrill, C. D. Density-fitted Open-shell Symmetry-adapted Perturbation Theory and Application to Π-stacking in Benzene Dimer Cation and Ionized DNA Base Pair Steps. *J. Chem. Phys.* 2016, *145*, 134106, DOI: 10.1063/1.4963385

12 Podeszwa, R.; Bukowski, R.; Szalewicz, K. Potential Energy Surface for the Benzene Dimer and Perturbational Analysis of Π- Π Interactions. *J. Phys. Chem. A* 2006, *110*, 10345– 10354, DOI: 10.1021/jp064095o

13 Sinnokrot, M. O.; Sherrill, C. D. Highly Accurate Coupled Cluster Potential Energy Curves for the Benzene Dimer: Sandwich, T-shaped, and Parallel-displaced Configurations. *J. Phys. Chem. A* 2004, *108*, 10200– 10207, DOI: 10.1021/jp0469517

14 Ehrlich, S.; Moellmann, J.; Grimme, S. Dispersion-corrected Density Functional Theory for Aromatic Interactions in Complex Systems. *Acc. Chem. Res.* 2013, *46*, 916– 926, DOI: 10.1021/ar3000844

15 Corminboeuf, C. Minimizing Density Functional Failures for Non-covalent Interactions Beyond Van Der Waals Complexes. *Acc. Chem. Res.* 2014, *47*, 3217– 3224, DOI: 10.1021/ar400303a

16 Rezáč, J.; Nachtigallová, D.; Mazzoni, F.; Pasquini, M.; Pietraperzia, G.; Becucci, M.; Müller-Dethlefs, K.; Hobza, P. Binding Energies of the Π-Stacked Anisole Dimer: New Molecular Beam—Laser Spectroscopy Experiments and CCSD (T) Calculations. *Chem. - Eur. J.* 2015, *21*, 6740– 6746, DOI: 10.1002/chem.201406134

17 Radloff, W.; Stert, V.; Ritze, H.-H.; Freudenberg, T. Ionization Potentials and Fragmentation Thresholds of the Heteroclusters Benzene-(SF6) M, M= 1–4. *Chem. Phys. Lett.* 1993, *205*, 171–177, DOI: 10.1016/0009-2614(93)89224-6

18 Petek, H.; Bell, A. J.; Choi, Y. S.; Yoshihara, K.; Tounge, B. A.; Christensen, R. L. The 2 1 A G State of Trans, Trans-1, 3, 5, 7-octatetraene in Free Jet Expansions. *J. Chem. Phys.* 1993, *98*, 3777– 3794, DOI: 10.1063/1.464056

19 Misaizu, F.; Houston, P. L.; Nishi, N.; Shinohara, H.; Kondow, T.; Kinoshita, M. Formation of Protonated Ammonia Cluster Ions: Two-color Two-photon Ionization Study. *J. Chem. Phys.* 1993, *98*, 336– 341, DOI: 10.1063/1.464626

20 Okuyama, K.; Cockett, M. C.; Kimura, K. Observation of Torsional Motion in the Ground-state Cation of Jet-cooled Tolane by Two-color Threshold Photoelectron Spectroscopy. *J. Chem. Phys.* 1992, *97*, 1649– 1654, DOI: 10.1063/1.463153

21 Wessel, J.; Beck, S.; Highstrete, C. Excitonic Interaction in the Fluorene Dimer. *J. Chem. Phys.* 1994, *101*, 10292– 10302, DOI: 10.1063/1.467909

22 Reilly, N.; Ivanov, M.; Uhler, B.; Talipov, M.; Rathore, R.; Reid, S. A. First Experimental Evidence for the Diverse Requirements of Excimer Vs Hole Stabilization in Π-Stacked Assemblies. *J. Phys. Chem. Lett.* 2016, *7*, 3042– 3045, DOI: 10.1021/acs.jpclett.6b01201

23 Uhler, B.; Ivanov, M. V.; Kokkin, D.; Reilly, N.; Rathore, R.; Reid, S. A. Effect of Facial Encumbrance on Excimer Formation and Charge Resonance Stabilization in Model Bichromophoric Assemblies. *J. Phys. Chem. C* 2017, *121*, 15580– 15588, DOI: 10.1021/acs.jpcc.7b04255

24 Mazzoni, F.; Pasquini, M.; Pietraperzia, G.; Becucci, M. Binding Energy Determination in a Π-stacked Aromatic Cluster: The Anisole Dimer. *Phys. Chem. Chem. Phys.* 2013, *15*, 11268– 11274, DOI: 10.1039/c3cp50191d

25 Wang, W.; Sun, T.; Zhang, Y.; Wang, Y.-B. The Benzene-naphthalene Complex: A More Challenging System Than the Benzene Dimer for Newly Developed Computational Methods. *J. Chem. Phys.* 2015, *143*, 114312, DOI: 10.1063/1.4931121

26 Perdew, J. P.; Ernzerhof, M.; Burke, K. Rationale for Mixing Exact Exchange with Density Functional Approximations. *J. Chem. Phys.* 1996, *105*, 9982– 9985, DOI: 10.1063/1.472933

27 Adamo, C.; Barone, V. Toward Reliable Density Functional Methods Without Adjustable Parameters: The PBE0 Model. *J. Chem. Phys.* 1999, *110*, 6158– 6170, DOI: 10.1063/1.478522

28 Grimme, S.; Antony, J.; Ehrlich, S.; Krieg, H. A Consistent and Accurate Ab Initio Parametrization of Density Functional Dispersion Correction (DFT-D) for the 94 Elements H-Pu. *J. Chem. Phys.* 2010, *132*, 154104, DOI: 10.1063/1.3382344

29 Adamo, C.; Barone, V. Toward Reliable Adiabatic Connection Models Free From Adjustable Parameters. *Chem. Phys. Lett.* 1997, *274*, 242– 250, DOI: 10.1016/S0009-2614(97)00651-9

30 Talipov, M. R.; Boddeda, A.; Timerghazin, Q. K.; Rathore, R. Key Role of End-capping Groups in Optoelectronic Properties of Poly-p-phenylene Cation Radicals. *J. Phys. Chem. C* 2014, *118*, 21400– 21408, DOI: 10.1021/jp5082752
31 Wang, D.; Talipov, M. R.; Ivanov, M. V.; Rathore, R. Energy Gap Between the Poly-p-phenylene Bridge and Donor Groups Controls the Hole Delocalization in Donor–Bridge–Donor Wires. *J. Am. Chem. Soc.* 2016, *138*, 16337– 16344, DOI: 10.1021/jacs.6b09209
32 Cammi, R.; Tomasi, J. Counterpoise Corrections to the Evaluation of the Bimolecular Interaction Energy Components. *Theor. Chim. Acta* 1986, *69*, 11– 22, DOI: 10.1007/BF00526288
33 Cammi, R.; Bonaccorsi, R.; Tomasi, J. Counterpoise Corrections to the Interaction Energy Components in Bimolecular Complexes. *Theor. Chim. Acta* 1985, *68*, 271– 283, DOI: 10.1007/BF00527535
34 Krylov, A. I. Equation-of-motion Coupled-cluster Methods for Open-shell and Electronically Excited Species: The Hitchhiker's Guide to Fock Space. *Annu. Rev. Phys. Chem.* 2008, *59*, 433– 462, DOI: 10.1146/annurev.physchem.59.032607.093602
35 Ditchfield, R.; Hehre, W. J.; Pople, J. A. Self-consistent Molecular-orbital Methods. IX. An Extended Gaussian-type Basis for Molecular-orbital Studies of Organic Molecules. *J. Chem. Phys.* 1971, *54*, 724– 728, DOI: 10.1063/1.1674902
36 Dunning, T. H., Jr Gaussian Basis Sets for Use in Correlated Molecular Calculations. I. The Atoms Boron Through Neon and Hydrogen. *J. Chem. Phys.* 1989, *90*, 1007– 1023, DOI: 10.1063/1.456153
37 Yanai, T.; Tew, D. P.; Handy, N. C. A New Hybrid Exchange–correlation Functional Using the Coulomb-attenuating Method (CAM-B3LYP). *Chem. Phys. Lett.* 2004, *393*, 51– 57, DOI: 10.1016/j.cplett.2004.06.011
38 Zhao, Y.; Truhlar, D. G. The M06 Suite of Density Functionals for Main Group Thermochemistry, Thermochemical Kinetics, Noncovalent Interactions, Excited States, and Transition Elements: Two New Functionals and Systematic Testing of Four M06-class Functionals and 12 Other Functionals. *Theor. Chem. Acc.* 2008, *120*, 215– 241, DOI: 10.1007/s00214-007-0310-x